Physical and Engineering Sciences in Medicine (2021) 44:1321–1329
https://doi.org/10.1007/s13246-021-01064-5

SCIENTIFIC PAPER

Analysis of normal lung irradiation in radiosurgery treatments: a comparison of lung optimized treatment (LOT) on cyberknife, 4D target volume on helical tomotherapy, and DIBH on linear accelerator

Raghavendra Holla[1] · D. Khanna[2] · V. K. Sathiya Narayanan[1] · Deb Narayan Dutta[3]

Received: 10 September 2020 / Accepted: 12 October 2021 / Published online: 1 November 2021

Abstract
Quantitative retrospective analysis of the normal lung irradiation due to the variations of the ITV volume based on the techniques used for upper lobe (UL), mid lobe (ML), and lower lobe (LL) lung tumours when used with 2-view, 1-view, 0-view based LOT technique on Cyberknife, AveIP on Helical Tomotherapy, and DIBH on VMAT systems. In the treatment of lung tumours, patients medically inoperable or those who are unwilling to undergo surgery have the option to be treated using radiation therapy. There are many motion control techniques available for the treatment of the moving target, such as movement encompassment, respiratory gating, breath-hold, motion reduction, and tumour monitoring. ITV generation is dependent on technique and hence the volume of the PTVs will differ based on the technique used. This study aimed to determine the influence of these ITVs on the irradiated normal lung volume for UL, ML, and LL lung tumours for 23 patients. The mean difference in the PTV volumes generated with the 0-view technique was significant with that of 2-view and DIBH techniques (p-value < 0.04). The mean difference in the PTV volumes generated by 2-view and DIBH was small for UL, ML, and LL tumours. V_5 of the combined lung with the 0-view method was 5% compared to the 2-view method for UL tumours (p-value = 0.04) and the same was 9.5%, and 16.8% for ML and LL tumours (p-value < 0.04). In contrast to all other techniques, lung volume parameters V_5, V_{10}, $V_{20,}$ and V_{30} for the 0-view technology were consistently higher irrespective of the tumour location in the lung. The observed maximum mean lung dose (MLD) was 6.2 Gy ± 2.7 Gy with the 0-view technique and the minimum was 3.85 Gy ± 1.75 Gy with the DIBH technique. The difference in MLD between DIBH and 2-view was negligible (p-value = 0.67). The MLD increased for LL tumours from 4 Gy to 6.5 Gy from the 2-view to 0-view technique (p-value = 0.009). There was a significant increase in MLD for LL tumours with the 0-view technique compared to AveIP (1.9 Gy, p-value = 0.04) and DIBH (2.0 Gy, p-value = 0.003) technique. For ML and UL tumours, except for 0-view and 1-view, the difference in the MLD between the rest of the methods was not significant (p-value > 0.11). In the treatment of lung tumour patients with SBRT, this study has demonstrated 2-view with Cyberknife and DIBH with VMAT treatment techniques have optimal normal lung tissue sparing. There was a significant increase in the average lung volume receiving 5%,10%, 20%, and 30% dose when comparing the 1-view, 0-view, AveIP, and DIBH techniques to the 2-view technique. However, DIBH with VMAT was dosimetrically advantageous for ML and LL tumours, while providing significantly shorter treatment times than any other technique studied.

Keywords Robotic radiosurgery · Lung tumour · DIBH · AveIP · Helical tomotherapy · VMAT

Introduction

Radiosurgery is the preferred treatment option for most inoperable lung tumours such as NSCLC [1]. The selection of the correct radiation technique is essential to achieve a high therapeutic ratio, ensuring adequate dose coverage for moving targets. With the advent of newer technology, there has been a rapid increase in the use of lung radiosurgery for both early-stage lung cancer and metastatic lung cases

✉ Raghavendra Holla
raghavendra.holla@gmail.com

[1] Ruby Hall Clinic, Pune, Maharashtra 411001, India

[2] Department of Physics, Karunya Institute of Technology and Sciences, Coimbatore 641114, India

[3] Department of Radiation Oncology, Amrita Institute of Medical Sciences, Amrita Vishwa Vidyapeetham, Kochi, India

[2]. Careful selection of the motion management strategies is necessary for the treatment of lung tumour and the selection should be based on clinical relevance. There are several motion management strategies available for these treatments such as motion encompassment, respiratory gating, breath-hold, motion mitigation, abdominal compression, and tumour tracking. The use of these techniques for lung tumour treatment has its advantages and disadvantages.

In the motion encompassment technique, the uncertainty of respiratory motion is managed by encompassing the entire range of tumour motion in the treated volume which mitigates the risk of missing the target. This is done by identifying the complete extent of tumour motion by incorporating all the potential tumour locations as part of the treatment volume. This is accomplished by 4D CT scanning in which the 4D CT data sets are created by acquiring separate CT images at discrete phases of the respiratory cycle [3].

In the breath-hold technique, the patient holds the breath at a planned respiratory phase with the aid of instruments such as active breathing control (ABC) device (Elekta Medical System, Sweden) or real-time position management (RPM) (Varian Medical Systems, Palo Alto, United States). The tumour volume is temporarily immobilized in a planned respiratory phase of the breathing and CT images are acquired. The treatment plans are generated using these breath-hold images. The planned respiratory phase for breath-holding can be at deep-inspiration (DIBH), normal inspiration, or end-expiration (deep expiration breath-hold (DEBH)) [4–8].

In the respiratory gating technique, the treatment beam is turned "on" during a specific pre-determined phase or amplitude portion of a breathing cycle, whereas, the patient is allowed to breathe with no constraints. When the tumour volume moves out of the gating window, the radiation beam will be turned off until it returns inside the gating window. The selection of a proper gating window plays an important role in the accuracy and efficiency of dose delivery. A very small gating window is ideal for an accurate dose delivery since it effectively freezes the tumour motion but at the cost of prolonged treatment time.

In real-time tumour tracking, the position of the tumour during organ motion is tracked on a real-time basis with the help of surgically implanted radiopaque fiducials implanted close to, or, inside the tumour or lesion in a minimally invasive interventional procedure [9–12]. These implanted fiducials are made of gold or other radiopaque metals, typically of the size between 1 and 5 mm.

During Cyberknife treatment, the patient wears a tightly fitting vest that has three infrared light-emitting diodes. A linear or quadratic correlation model is generated to relate the position signals of the LEDs to the internal fiducial marker locations using two orthogonal radiographs of the patient on the treating table obtained by the X-ray system. This model is used as a prediction model for predicting the fiducial marker position on a real-time basis. The Cyberknife treatment will interrupt if the predicted fiducial position by the model differs from the position indicated by the X-ray system by 5 mm. Although the X-rays are taken every few seconds the model enables near-continuous tracking of the tumour. The correlation error between the prediction model to the actual position of the tumour was found to differ in matching anatomic directions by no more than 1 mm [13].

The option in the Cyberknife system for eliminating the fiducial marker for tracking the lung tumour used in lung optimized treatment (LOT) is a 2-view modality with dynamic tumour tracking by using the 2D images from orthogonally placed X-ray tubes. In 1-view modality, the tumour is visible in only one of the X-ray projections and dynamic tumour tracking compensates the target motion only in the detectable plane. Non-visible motion is compensated with an internal target volume (ITV)-based strategy. When the tumour is not visible in both the images, the 0-view modality by ITV based approach is used.

In 2-view tracking, the tumour margins are minimal since tumour can be localized using both the orthogonal images. The robot coordinates are based on the gross tumour detected in both the images and the 3D coordinates derived from these two images. If the tumour is very close to the heart or mediastinum, it is not visible or differentiable from the surrounding soft tissue. In these cases, the tumour is not visible on both detectors. Then the ITV from the end of the exhale and end of inhale CT images are derived with additional margins in all the directions, and the robot coordinates are derived from the spine tracking volumes. In this case, the normal lung tissue irradiation is very high depending on the size and position of the tumour. For LOT, a high-density isolated tumour in the middle of the low-density lung volume is ideal. However, the selection of the appropriate method is done only after a proper simulation plan with the patient.

These different techniques used in lung tumour treatment have their pros and cons. The large margin expansions to encompass the entire tumour motion sometimes require a dose reduction to spare normal tissue depending on the location of the tumour [14]. Because the process for generating the ITV differs between methodologies, the resulting planning target volume (PTV) differs as well. These ITVs will have distinct effects on the irradiated lung volume. With all of these delivery mechanisms influencing clinical outcomes, there will be a distinct proportion of 'high dose' and 'low dose' spill regions. Several authors have compared the treatment plans utilizing various motion management strategies [15–17]. However, no prospective comparison study has yet been conducted that compares the LOT of Cyberknife, DIBH with volumetric modulated arc therapy (VMAT), and average intensity projection images (AveIP) in HT in a consistent study design with lung dose sparing as an objective.

The goal of this study was to do a retrospective quantitative analysis of normal lung irradiation owing to differences in ITV volume based on techniques employed for UL, ML, and LL lung tumours.

Materials and Methods

Twenty-three patients with either early lung cancer or small lung metastasis were considered for this study. All the patients were planned for robotic radiosurgery treatment as per the standard robotic radiosurgery planning guideline of the institution. During the simulation process, CT images were acquired with the respiratory phase at the end of the exhale and end of inhale as required for the Cyberknife LOT technique using the Optima 580 W CT scanner (GE Medical Systems, Chicago, USA). The breath hold images in the deep inspirational phase of the breathing were used as DIBH images for VMAT planning. The AveIP images were generated from cine CT images using 10 phase binned image sets sorted and reconstructed using a phase binning reconstruction based on the respiratory profile provided by smart deviceless system (GE medical systems, Chicago, USA). For all the techniques mentioned above, the CT acquisitions were done with 0.625 mm slice thickness with a tube current of 200 mA, and a voltage of 120 kV. The end of inhale, end of exhale, and AveIP CT images were transferred to the Precision treatment planning system (version 2.0, Accuray Inc., Madison, WI) for generating ITV and then treatment plans were generated for Cyberknife and HT systems. The DIBH imagers were transferred to Monaco treatment planning system (Elekta, Stockholm, Sweden). The target delineation including gross tumour volume (GTV), clinical target volume (CTV), ITV, and PTVs was performed on their respective images. On each patient, ITVs were created utilising 2-view, 1-view, and 0-view approaches for Cyberknife planning. A uniform margin of 3 mm was applied to ITV for creating PTV for a 2-view technique. In the case of 0 -view an additional margin of 2 mm making a total of 5 mm from the ITV was applied. For the 1-view technique, a non-uniform margin of 3 mm and 5 mm in the plane of tracking and out of the plane was applied respectively. These margins are based on quantitative verification of the adequacy of the PTV margins applied in CyberKnife LOT treatments [18]. The PTVs for DIBH and AveIp planning were obtained by adding a uniform margin of 5 mm to the ITVs, which was used to compensate for setup uncertainties and residual respiratory motion not represented by 4D CT as per our institutional routine practice. The combined normal lungs were automatically segmented using a threshold algorithm at the respective planning system. The detailed patient characteristics of the 23 patients were summarized in Table 1.

Table 1 Patient characteristics

Characteristic	Number (N)
Sex	
Male	16
Female	7
Age (years)	
Range	34–81
Median age	67
Histology	
NSCLC	9
Mets	14
Primary tumour location	
UL	13
LL	6
ML	4

NSCLC non-small cell lung carcinoma, *UL* upper lobe, *LL* lower lobe, *ML* middle lobe

Treatment Planning

A tumour dose of 45 Gy in 5 fractions was prescribed to the PTV in all the plans. The plan characteristics in various planning systems were listed in Table 2 below. The Cyberknife plans were created using an IRIS beam collimation system, whereas the HT plans used an MLC leaf width of 0.625 cm projected to the isocenter. The VMAT plans were generated with APEX MLC with a 2.5 mm resolution at the isocenter. For Cyberknife plans, the minimum collimator size was maintained above 10 mm. HT planes with a dynamic jaw size of 2.51 cm field width with a pitch of 0.2 and a modulation factor of 2.0 were developed in helical delivery mode. The optimization algorithms used by the Cyberknife, HT, and VMAT treatment planning systems differ. Within each treatment planning system, however, the planning constraints were set the same to obtain the largest target coverage.The overlaid PTV contours for UL, ML, and LL tumour are shown on DIBH images in Fig. 1.

Plan Comparison

For all of the techniques, single point matrices such as mean lung dose (MLD), V_5 (volume of the combined lung receiving 5 Gy or higher—PTV volume), V_{10} (volume of the combined lung receiving 10 Gy or higher—PTV volume), V_{20} (volume of the combined lung receiving 20 Gy or higher—PTV), V_{30} (volume of the combined lung receiving 30 Gy or higher—PTV) were calculated. Further, the dose received by the 10%, 20%, and 50% of the combined normal lung volume was analyzed.

The dose distribution on PTV was evaluated by using parameters such as conformity index (CI) [19], homogeneity

Table 2 Treatment planning characteristics

Technique	Treatment planning system	Planning target	Dose calculation resolution	Beam energy	Calculation algorithm
2-View	Precision 2.0	ITV from end of exhale CT images + 3 mm margin for PTV	$1 \times 1 \times 1$ mm^3	6 MV unflattenned	Montecarlo
1-View	Precision 2.0	ITV from end of exhale CT images + 3 mm margin for PTV in viewing plan and + 5 mm in non-viewing plan	$1 \times 1 \times 1$ mm^3	6 MV unflattenned	Montecarlo
0-View	Precision 2.0	ITV from end of exhale CT images + 5 mm margin for PTV	$1 \times 1 \times 1$ mm^3	6 MV unflattenned	Montecarlo
AveIP	Precision 2.0	ITV from 4D AveIP CT images + 5 mm margin for PTV	$1 \times 1 \times 1$ mm^3	6 MV unflattenned	CC superposition
DIBH	Monaco 5.1	ITV from DIBH CT images + 5 mm margin for PTV	$1 \times 1 \times 1$ mm^3	6 MV flattenned	Montecarlo

ITV internal target volume, *PTV* planning target volume, *AveIP* average intensity projection, *DIBH* deep inspirational breath hold

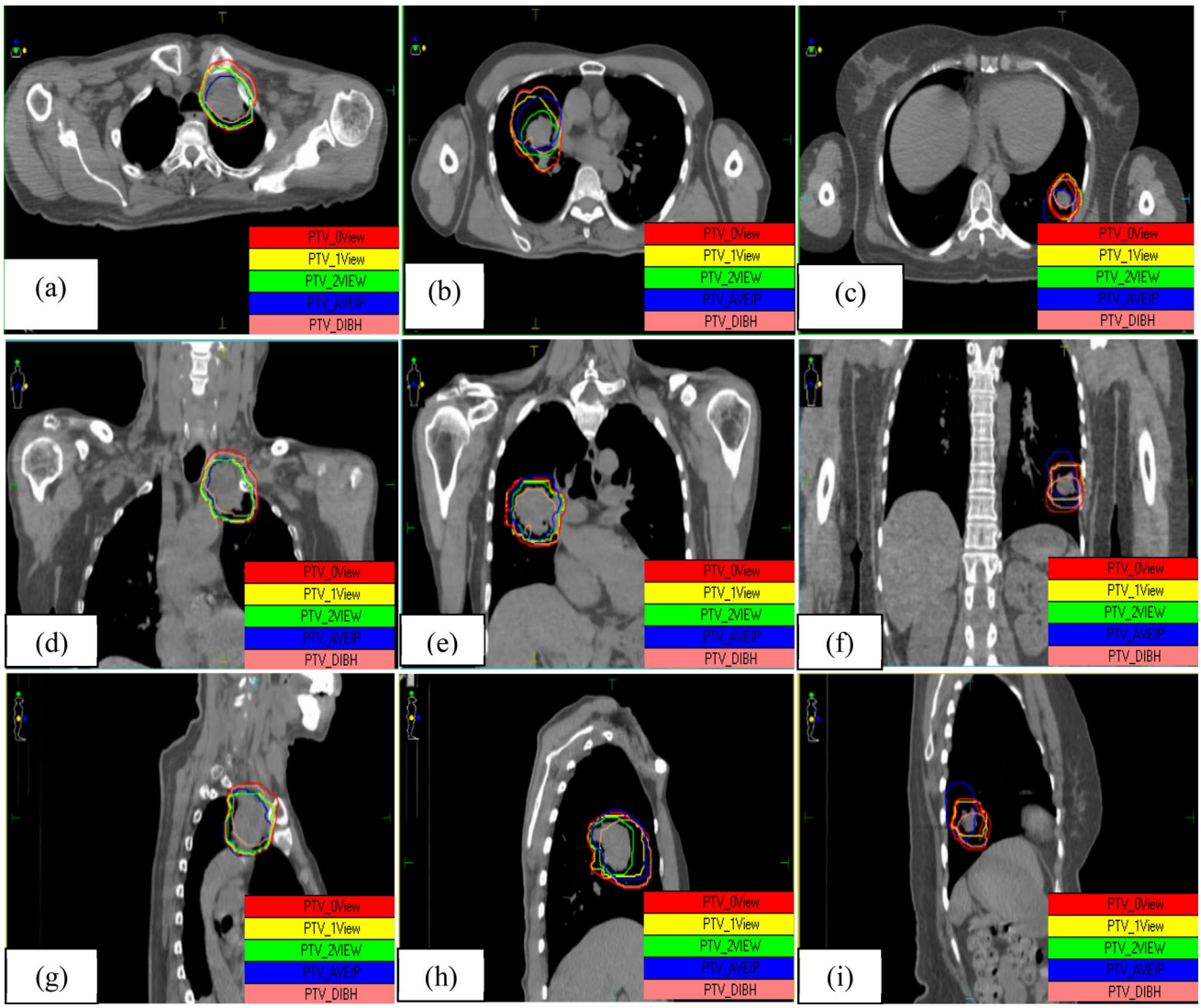

Fig. 1 CT images showing the overlay of PTV derived from ITV in: transverse images for tumours in **a** UL, **b** ML, **c** LL for left, right and left lung tumours: coronal plan images **d** UL, **e** ML, **f** LL and sagittal plan images **g** UL, **h** ML, **i** LL. The PTV contours drawn on their respective image sets overlaid on DIBH images in red, yellow, green, blue and orange colors for 0-view, 1-view, 2-view, AveIP and DIBH techniques respectively

index (HI) [20], and gradient index (GI) [21]. The CI was calculated according to the following equation:

$$\mathrm{CI} = \frac{(V_{ROI,pres})^2}{V_{ROI} X V_{body,pres}}$$

where $V_{ROI,\ pres}$ is the volume of PTV covered by the prescription dose, V_{ROI} is the volume of PTV, and $V_{body,\ pres}$ is the total volume covered by the prescription dose.

The heterogeneity index (HI) was calculated as:

$$HI = \frac{D_2 - D_{98}}{D_{pres}}$$

where D_2 and D_{98} correspond to radiation doses delivered to 2% and 98% of the PTV, respectively. D_{pres} is the prescription dose to PTV. The gradient index was calculated as the ratio of the volume of half the prescription isodose to the volume of the prescription isodose [21].

Statistical Analysis

SPSS ver. 19.0 (SPSS Inc., Chicago, IL, USA) was used for the statistical analysis. The dosimetric differences in all the techniques were compared to the 2-view techniques using an independent Student t-test with the hypotheses of (H0: $\mu 1 = \mu 2$) for the mean evaluated volume (μ) among different techniques such as mean lung dose (MLD), V_5, V_{10}, V_{20}, and V_{30}, at a confidence level of 95% ($\alpha = 0.05$). A *p*-value less than 0.05 is considered statistically significant.

Results

The average dose received by 10%, 20%, and 50% of the combined normal lung volume classified based on the tumour in UL, ML, and LL of the lung is shown in Table 3. The dose received by 10% of the lung volume was less with the 2-view technique for UL and LL tumours. For ML tumours $D_{10\%}$, $D_{20\%,}$ and $D_{50\%}$ were minimum with the DIBH technique.

The average PTV volume created using the 0-view technique was 80.5 cc, 53.2 cc with the 1-view technique, 33.2 cc with the 2-view methodology, 51 cc with the AveIP approach, and 48.7 cc with the DIBH methodology. The mean difference in PTV volumes obtained with the 0-view approach compared to those obtained with the 2-view and DIBH procedures was significant (p-value < 0.04). The average PTV volume using 2-view technique was lower compared with 1-view (p value = 0.21), 0-view (p-value = *0*.006), AveIP (p-value = 0.37) and DIBH (p value = 0.53). For UL, ML, and LL tumours, the mean difference in PTV volumes obtained by 2-view and DIBH was insignificant. For UL and ML tumours, the difference in PTV volume between AveIP and DIBH was minimal. (< 1 cc).

Table 3 The average dose received by 10%, 20%, and 50% of the combined lung volume for 2-view, 1-view, 0-view, AveIP, and DIBH techniques classified into midlobe (ML), upperlobe (UL), and lowerlobe (LL) tumours

	Dose in Gy				
	2-view	1-view	0-view	AveIP	DIBH
$D_{10\%}$					
ML	17.5	20.2	24.2	17.8	17.0
UL	9.6	11.6	13.3	11.8	11.3
LL	9.8	13.9	18.0	13.6	11.3
$D_{20\%}$					
ML	9.9	11.7	14.8	9.4	7.6
UL	4.1	5.2	5.9	4.9	4.5
LL	4.8	6.6	9.1	5.2	4.4
$D_{50\%}$					
ML	2.6	3.1	3.9	2.1	1.1
UL	1.3	1.4	1.8	1.1	0.7
LL	1.5	2.0	2.8	1.8	0.6

The 0-view method increased V_5 of the combined lung by 5% compared to the 2-view technique for UL tumours (p value = 0.04), 9.5% for ML (p value = 0.04), and 16.8% for LL tumours (p value = 0.04). In contrast to all other techniques, for UL, ML, and LL tumours, lung volume parameters V_5, V_{10}, $V_{20,}$ and V_{30} for the 0-view technology were consistently higher. V_5 was less in DIBH technique than the 2-view technique for ML tumours by 4.2%. In comparison with other techniques shown in Fig. 2, the volume parameters V_{10}, V_{20} andV_{30} were constantly lower in DIBH technology.

The observed maximum mean lung dose (MLD) was 6.2 Gy ± 2.7 Gy with a 0-view technique and the minimum was 3.85 Gy ± 1.75 Gy with the DIBH technique as shown in Fig. 3. The difference in MLD between DIBH and 2-view was negligible (p-value = 0.67). For LL tumours, the MLD increased from 4 to 6.5 Gy from the 2-view to 0-view technique (p-value = 0.009) (Fig. 3). Except for 0-view and 1-view, the difference in MLD was not significant for ML and UL tumours. (p-value > 0.11).

All five techniques resulted in similar dose conformity but the homogeneity was better with VMAT and HT plans as shown in Table 4. In contrast, VMAT reduced the delivery time by 94% and 80% compared to Cyberknife and HT. When compared to Cyberknife and HT, VMAT reduced monitor unit (MU) by 91% and 89%, respectively. The gradient index was high for DIBH (5.4 ± 0.6) and AveIP (5.9 ± 0.6) techniques compared to Cyberknife 2-view (3.5 ± 0.8) plans.

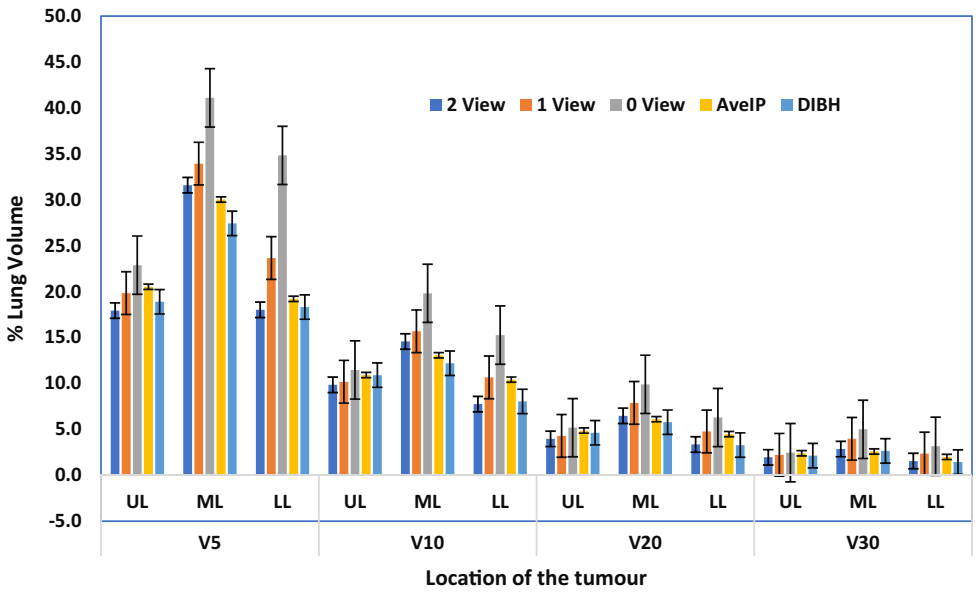

Fig. 2 Average percentage lung volume receiving 5 Gy, 10 Gy, 20 Gy, and 30 Gy dose between 2-view, 1-view, 0-view, AveIP, and DIBH techniques with their standard deviation, classified based on the location of the tumour in UL, ML, and LL of the lung

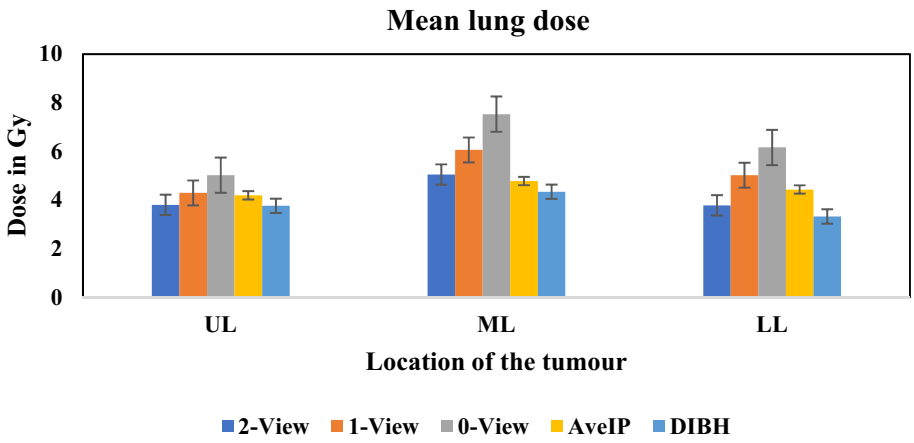

Fig. 3 Average MLD with standard deviation for 2-view, 1-view, 0-view, AveIP, and DIBH techniques classified based on the location of the tumour in UL, ML, and LL of the lung

Table 4 The characteristics of target dose distributions obtained for the 2-view, 1-view, 0-view, AveIP in HT, and DIBH in Vmat

	2-View	1-View	0-View	AveIP in HT	DIBH in VMAT
Monitor units	36,221 ± 11,043	38,93 ± 8336	41,473 ± 8159	20,494 ± 6282	2201 ± 803
Beam ON in seconds	3071 ± 478	3254 ± 311	3106 ± 445	1042 ± 319	205 ± 55
Conformity index (CI)	1.20 ± 0.13	1.20 ± 0.1	1.10 ± 0.1	1.10 ± 0.10	1.10 ± 0.1
Homogeneity index (HI)	1.20 ± 0.1	1.30 ± 0.1	1.30 ± 0.1	1.10 ± 0.02	1.12 ± 0.03
Gradient Index (GI)	3.5 ± 0.8	4.2 ± 0.7	4.6 ± 0.5	5.9 ± 0.6	5.4 ± 0.6

Discussion

Both high dose and low dose spillage play a role in radiation-induced lung damage. Early lung tissue necrosis is mostly caused by high dose spillage, while late interstitial fibrosis is caused by low dose spillage. In this study, clinically treated patients in the full patient cohort and all patient subgroups, such as UL, ML and LL involvement, were compared directly between three of these modalities: Cyberknife, AveIP in HT, and DIBH in VMAT. 115 treatment plans were created for 23 lung patients to provide conformal dose distributions with clinically acceptable doses to the OAR. The ITVs used by different delivery techniques for treating lung tumours were investigated to see how they influenced normal lung doses. The planner

dependent variability of the generated plans has to be considered while comparing different plans using different dose calculation algorithms. In this study, all of the plans were developed by the same physicist at planning systems to eliminate the planner-dependent variability of the created plans. The influence of different dose calculation algorithms used in treatment planning systems is apparent predominantly in the target periphery and dose-buildup region while maintaining the same OAR dose parameters [22]. This could be because different plan optimization techniques use different normal structure constraints to produce the same dose volume values. However, in this study we maintained the same target goals in all the planning systems leading to different best achievable normal structure constraints. Further the patient specific point dose measurements were carried out to compare the dose differences due to the calculation algorithm used in treatment planning systems. This was carried out by overlaying the accepted treatment plan on a homogeneous phantom. For point dose, 0.125 cc cylindrical ionization chamber was used to measure the dose at the center of homogenous cylindrical phantom. The cumulative dose was measured and compared to the dose calculated to the same point in the phantom plan. The measured absolute point dose measurements agreed within 2% for all the modalities.

We observed the distinct dosimetric advantage of the 2-view and VMAT plans over 1-view, 0-view, and HT at high-dose (V_{30}) regions. In this study, HI for the PTVs were higher in the Cyberknife plan than in the VMAT and HT plans. VMAT and HT, in other words, have an advantage in terms of achieving homogeneous dose distributions in the tumour region. However, while hot spots inside PTVs are clinically acceptable, homogenous dose distribution in the tumour region should not be simply seen as an advantage for SBRT.The gradient indices for Cyberknife plans were smaller than VMAT and HT showing significant difference in dose falloff between Cyberknife and other techniques.

Except for the 0-view approach at Cyberknife, there was no absolute dosimetric advantage to choosing between Cyberknife, HT, or VMAT procedures for SBRT of the lung in UL tumours. The 0-view technique is inferior to all other procedures regardless of the tumour location in the lung, as the mean lung dose for UL, ML, and LL lung tumours was 5.02 Gy, 7.53 Gy, and 6.16 Gy, respectively.This is mainly due to the additional margin of 2 mm used to generate the PTV. The 2-view and DIBH techniques are advantageous when treating ML and LL lung tumours despite the fact that the PTV margin for DIBH was increased by 2 mm. The conformance index did not differ across the 5 techniques, despite the fact that the Cyberknife plans resulted in longer treatment times and more monitor units. The VMAT plans have the shortest treatment times and the lowest monitor units.

As shown in Fig. 4, for a tumour in the LL of the lung, the 5 Gy volume (V_{5Gy}) for contralateral lung was minimal with Cyberknife plans than HT and VMAT plans. This increase

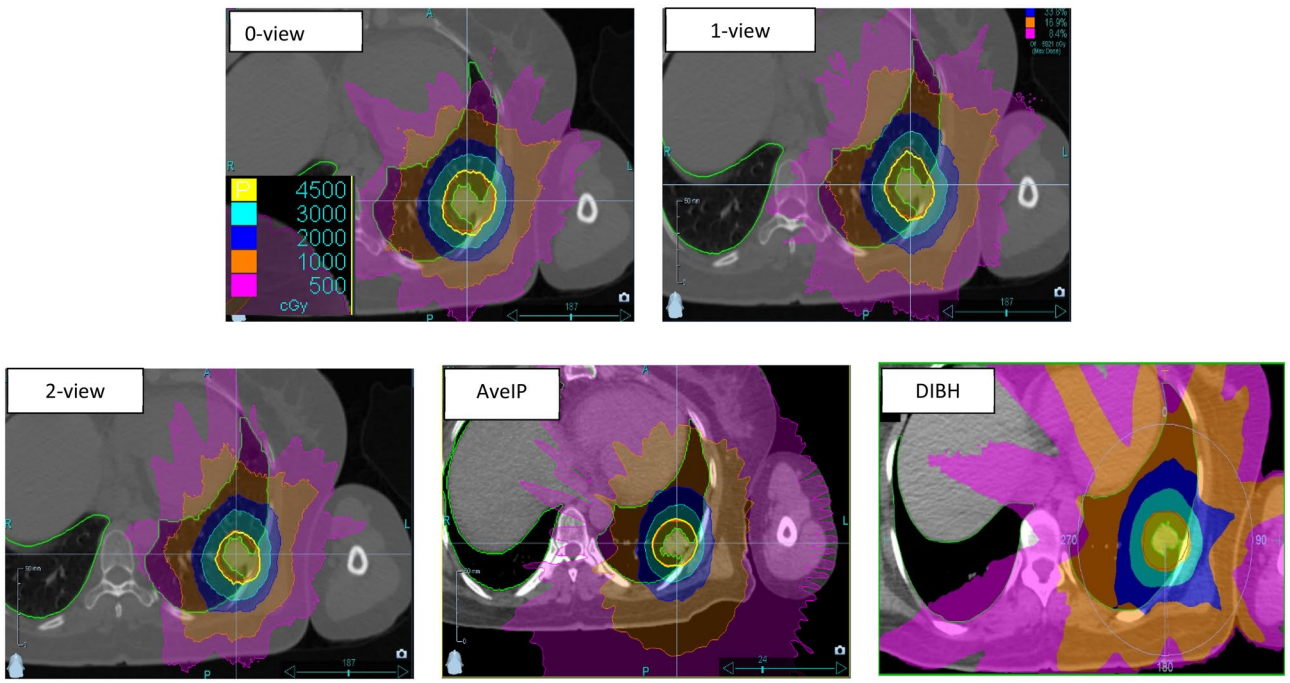

Fig. 4 Treatment plans in sagittal axis showing the isodose distributions for 0-view, 1-view, 2-view, AveIP, and DIBH images on Cyberknife, HT and VMAT plans. The 5 Gy isodose distribution on the contralateral lung can be seen

in HT and VMAT plans could be due to the beam entry through the opposite lung. During helical and arc therapy, the beam entry through the opposite lung was unavoidable. The 5 Gy dose volume in the ipsilateral lung was higher in Cyberknife than HT and VMAT plans. In Cyberknife, the optimizer restricts the beam entry through the contralateral side due to the reduced clearance between the patient surfaces to the machine to avoid a collision. This reduces the degrees of freedom of the optimizer resulting increased 5 Gy volume in the ipsilateral lung.

The dynamic tumour tracking during treatment delivery, which is a technology-specific capacity of the delivery systems, is another key consideration when comparing different treatment modalities for lung SBRT, specifically at Cyberknife. The target contours alter depending on whether or not dynamic tumour tracking is available, and therefore the volume of irradiated normal lung volume. The target volume for 0-view was always higher than for other techniques, and this difference was due to the tumour's position in the lung, such as UL, ML, or LL. The LL tumours move more than ML and UL tumours necessitating a bigger target volume for 0-view, 1-view, and AveIP techniques [23]. However, regardless of the location of the tumour, we kept the same ITV margin for 0-view and 1-view in our investigation, whereas the ITV volume generated in AveIP images is dependent on the total tumour volume excursion. Hence the ITV generated from AveIP images will be high if the tumour volume excursion is high, as it is in ML and LL tumours.

The choice of Lung Optimised Treatment is based on tumour visibility on 2D images from orthogonally positioned x-ray tubes. When multiple approaches such as VMAT, DIBH or HT are available at an institution, detailed normal tissue data aids in making a more informed decision about which approach to use. In this study we have compared 2-view, 1-view and 0-view methods of LOT with alternative approaches such as DIBH in VMAT and AvIP in HT to determine the most appropriate methodology based on the tumour location.

VMAT was found to provide more efficient treatment delivery by reducing the monitor units and delivery time. The Cyberknife was found to be the most inefficient and also takes additional time to generate a breathing model of the patient before each treatment.

Conclusions

This study demonstrated that 2-view with Cyberknife and DIBH with VMAT treatment techniques offer the best normal lung tissue sparing while treating lung cancer patients with SBRT. Although all plans were clinically acceptable in terms of target dose coverage, 2-view and DIBH surpassed all other techniques in terms of lower values for V_5, V_{10}, V_{20}, and V_{30} of normal lung irradiated. Further, the lower values for V_5, V_{10},V_{20} and V_{30} for the DIBH plan can be attributed partly to the larger lung volume in the deep inspiration breath hold scans.

There was a significant increase in the average lung volume receiving 5%, 10%, 20%, and 30% dose when comparing the 1-view, 0-view, AveIP, and DIBH techniques to the 2-view technique. However, DIBH with VMAT was dosimetrically advantageous for ML and LL tumours, while providing significantly shorter treatment times than any other technique studied.

Supplementary Information The online version contains supplementary material available at https://doi.org/10.1007/s13246-021-01064-5.

Funding None.

Data availability All data generated and analyzed during this study are included in this published article (and its supplementary information files).

Declarations

Conflict of interest The authors declare that they have no conflict of interest.

Ethical approval This study was approved by the Institutional ethical committee.

Informed consent obtained for research All participants provided written informed consent prior to enrolment in the study.

References

1. Guckenberger M, Krieger T, Richter A et al (2009) Potential of image-guidance, gating and real-time tracking to improve accuracy in pulmonary stereotactic body radiotherapy. Radiother Oncol 91:288–295
2. Franks KN, Jain P, Snee MP (2015) Stereotactic ablative body radiotherapy for lung cancer. Clin Oncol 27(5):280–289. https://doi.org/10.1016/j.clon.2015.01.006
3. Pan T, Lee TY, Rietzel E, Chen GT (2004) 4D-CT imaging of a volume influenced by respiratory motion on multislice CT. Med Phys 31(2):333–340. https://doi.org/10.1118/1.1639993
4. Rosenzweig KE, Hanley J, Mah D, Mageras G, Hunt M, Toner S, Burman C, Ling CC, Mychalczak B, Fuks Z, Leibel SA (2000) The deep inspiration breath-hold technique in the treatment of inoperable non-small-cell lung cancer. Int J Radiat Oncol Biol Phys 48(1):81–87. https://doi.org/10.1016/s0360-3016(00)00583-6
5. Glide-Hurst CK, Gopan E, Hugo GD (2010) Anatomic and pathologic variability during radiotherapy for a hybrid active breath-hold gating technique. Int J Radiat Oncol Biol Phys 77(3):910–917. https://doi.org/10.1016/j.ijrobp.2009.09.080
6. Stromberg JS, Sharpe MB, Kim LH, Kini VR, Jaffray DA, Martinez AA, Wong JW (2000) Active breathing control (ABC) for Hodgkin's disease: reduction in normal tissue irradiation with deep inspiration and implications for treatment. Int J Radiat Oncol

Biol Phys 48(3):797–806. https://doi.org/10.1016/s0360-3016(00)00681-7
7. Remouchmamps VM, Vicini FA, Sharpe MB, Kestin LL, Martinez AA, Wong JW (2003) Significant reductions in heart and lung doses using deep inspiration breath hold with active breathing control and intensity-modulated radiation therapy for patients treated with locoregional breast irradiation. Int J Radiat Oncol Biol Phys 55(2):392–406. https://doi.org/10.1016/s0360-3016(02)04143-3
8. Negoro Y, Nagata Y, Aoki T, Mizowaki T, Araki N, Takayama K, Kokubo M, Yano S, Koga S, Sasai K, Shibamoto Y, Hiraoka M (2001) The effectiveness of an immobilization device in conformal radiotherapy for lung tumour: reduction of respiratory tumour movement and evaluation of the daily setup accuracy. Int J Radiat Oncol Biol Phys 50(4):889–898. https://doi.org/10.1016/s0360-3016(01)01516-4
9. Shirato H, Shimizu S, Kunieda T, Kitamura K, van Herk M, Kagei K, Nishioka T, Hashimoto S, Fujita K, Aoyama H, Tsuchiya K, Kudo K, Miyasaka K (2000) Physical aspects of a real-time tumour-tracking system for gated radiotherapy. Int J Radiat Oncol Biol Phys 48(4):1187–1195. https://doi.org/10.1016/s0360-3016(00)00748-3
10. Shirato H, Harada T, Harabayashi T, Hida K, Endo H, Kitamura K, Onimaru R, Yamazaki K, Kurauchi N, Shimizu T, Shinohara N, Matsushita M, Dosaka-Akita H, Miyasaka K (2003) Feasibility of insertion/implantation of 2.0-mm-diameter gold internal fiducial markers for precise setup and real-time tumour tracking in radiotherapy. Int J Radiat Oncol Biol Phys 56(1):240–247. https://doi.org/10.1016/s0360-3016(03)00076-2
11. Shimizu S, Shirato H, Kitamura K, Shinohara N, Harabayashi T, Tsukamoto T, Koyanagi T, Miyasaka K (2000) Use of an implanted marker and real-time tracking of the marker for the positioning of prostate and bladder cancers. Int J Radiat Oncol Biol Phys 48(5):1591–1597. https://doi.org/10.1016/s0360-3016(00)00809-9
12. Adler JR, Chang SD, Murphy MJ, Doty J, Geis P, Hancock SL (1997) The cyberknife: a frameless robotic system for radiosurgery. Stereotactic Funct Neurosurg 69(1–4 Pt 2):124–128. https://doi.org/10.1159/000099863
13. Pepin EW, Wu H, Zhang Y, Lord B (2011) Correlation and prediction uncertainties in the cyberknife synchrony respiratory tracking system. Med Phys 38(7):4036–4044. https://doi.org/10.1118/1.3596527
14. Molitoris JK, Diwanji T, Snider JW, Mossahebi S, Samanta S, Badiyan SN, Simone CB, Mohindra P (2018) Advances in the use of motion management and image guidance in radiation therapy treatment for lung cancer. J Thorac Dis 10(Suppl 21):S2437–S2450. https://doi.org/10.21037/jtd.2018.01.155
15. Chin E, Loewen S, Nichol A, Otto K (2013) 4D VMAT, gated VMAT, and 3D VMAT for stereotactic body radiation therapy in lung. Phys Med Biol 58:749
16. Chin E, Otto K (2011) Investigation of a novel algorithm for true 4D-VMAT planning with comparison to tracked, gated and static delivery. Med Phys 38:2698–2707
17. Falk M, Pommer T, Keall P et al (2014) Motion management during IMAT treatment of mobile lung tumours—a comparison of MLC tracking and gated delivery. Med Phys 41:101707
18. Ricotti R, Seregni M, Ciardo D, Vigorito S, Rondi E, Piperno G, Ferrari A, Zerella MA, Arculeo S, Francia CM, Sibio D, Cattani F, De Marinis F, Spaggiari L, Orecchia R, Riboldi M, Baroni G, Jereczek-Fossa BA (2018) Evaluation of target coverage and margins adequacy during CyberKnife Lung Optimized Treatment. Med Phys 45(4):1360–1368. https://doi.org/10.1002/mp.12804
19. van't Riet A, Mak AC, Moerland MA et al (1997) A conformation number to quantify the degree of conformality in brachytherapy- and external beam irradiation: application to the prostate. Int J Radiat Oncol Biol Phys 37:731–736
20. Prescribing, recording, and reporting photon-beam intensity modulated radiotherapy (IMRT) Oxford: Oxford University Press, International Commission on Radiation Units and Measurements; 2010. ICRU Report 83.
21. Paddick I, Lippitz B (2006) A simple dose gradient measurement tool to complement the conformity index. J Neurosurg 105(Suppl):194–201. https://doi.org/10.3171/sup.2006.105.7.194
22. Chopra KL, Harkenrider MM, Emami B et al (2019) Impact of choice of dose calculation algorithm on PTV and OAR doses in lung SBRT. J Radiat Oncol 8:291–304. https://doi.org/10.1007/s13566-019-00399-7
23. Knybel L, Cvek J, Molenda L, Stieberova N, Feltl D (2016) Analysis of lung tumor motion in a large sample: patterns and factors influencing precise delineation of internal target volume. Int J Radiat Oncol Biol Phys 96(4):751–758. https://doi.org/10.1016/j.ijrobp.2016.08.008